Spectrochimica Acta Part A: Molecular and Biomolecular Spectroscopy 130 (2014) 230–237

Contents lists available at ScienceDirect

Spectrochimica Acta Part A: Molecular and Biomolecular Spectroscopy

journal homepage: www.elsevier.com/locate/saa

Synthetic aspects, spectral, thermal studies and antimicrobial screening on *bis*(*N*,*N*-dimethyldithiocarbamato-*S*,*S*′)antimony(III) complexes with oxo or thio donor ligands

H.P.S. Chauhan *, Jaswant Carpenter, Sapana Joshi

School of Chemical Sciences, Devi Ahilya University, Takshashila Campus, Khandwa Road, Indore 452001, India

HIGHLIGHTS

- Mixed *bis*(*N*,*N*-dimethyldithiocarbamato-*S*,*S*′)antimony(III) complexes.
- The complexes adopted distorted octahedral geometry with lone pair of electrons.
- These are crystalline in nature, nano-ranged and having monoclinic crystal system.
- Antimony sulfide was a final decomposition product upon thermal decomposition.
- These showed a greater or equal antimicrobial activity than the standard drugs.

GRAPHICAL ABSTRACT

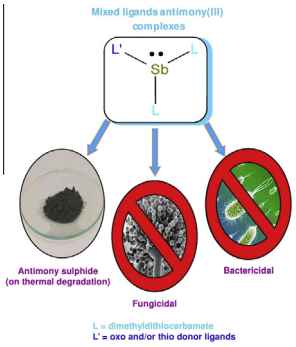

ARTICLE INFO

Article history:
Received 29 December 2013
Received in revised form 10 March 2014
Accepted 20 March 2014
Available online 13 April 2014

Keywords:
Antimony(III)
Dithiocarbamate
Thermogravimetric
Powder XRD
Antimicrobial
Antimony sulfide

ABSTRACT

The *bis*(*N*,*N*-dimethyldithiocarbamato-*S*,*S*′)antimony(III) complexes have been obtained by the reaction of chloro *bis*(*N*,*N*-dimethyldithiocarbamato-*S*,*S*′)antimony(III) with corresponding oxo or thio donor ligands such as sodium benzoate **1**, sodium thioglycolate **2**, phenol **3**, sodium 1-propanethiolate **4**, potassium thioacetate **5**, sodium salicylate **6**, ethane-1,2-dithiolate **7** and disodium oxalate **8**. These complexes have been characterized by the physicochemical [melting point, molecular weight determination and elemental analysis (C, H, N, S and Sb)], spectral [UV–Visible, FT-IR, far IR, NMR (^{1}H and ^{13}C)], thermogravimetric (TG & DTA) analysis, ESI-Mass and powder X-ray diffraction studies. Thermogravimetric analysis of the complexes confirmed the final decomposition product as highly pure antimony sulfide (Sb_2S_3) and powder X-ray diffraction studies show that the complexes are in lower symmetry with monoclinic crystal lattice and nano-ranged particle size (11.51–20.82 nm). The complexes have also been screened against some bacterial and fungal strains for their antibacterial and antifungal activities and compared with standard drugs. These show that the complexes have greater activities against some human pathogenic bacteria and fungi than the activities of standard drugs.

Introduction

Dithiocarbamates owe special significance due to their wide spread applications such as vulcanization additives, stabilizers for PVC, nitrogen–oxygen trapping agents, chelating agents of heavy

* Corresponding author. Tel.: +91 731 2460208 (office), mobile: +91 9826219748; fax: +91 731 2365782.
E-mail address: hpsc@rediffmail.com (H.P.S. Chauhan).

http://dx.doi.org/10.1016/j.saa.2014.03.054
1386-1425/

metals, lubricants and catalysts [1–4]. They have also been used as biologically active molecules [4,5–9] such as fungicides, bactericides, anticancer agents [10–12] and as arrestors of human immunodeficiency virus (HIV) infections such as AIDS [13–15]. The antimicrobial effect of dithiocarbamates has been reported to arise by the reaction of HS-groups with physiologically important enzymes by transferring the alkyl group of the dithioester to the HS-function of the enzyme [19,20].

These are versatile ligands with remarkable diversities in their bonding and coordination pattern with main group metals [16–21] and have been widely studied [1–4,5–9]. A number of metal dithiocarbamate complexes have been used in analytical chemistry [22], as antioxidants [23,24], polymer photo stabilizers [25] and precursor for creating sulfide film semiconductors [26]. Trivalent antimony compounds have also been used as drugs for the treatment of laishmaniasis span more than 50 years [27,28]. Antimony metal complexes containing Sb—S bonds have been widely used in industrial processes [29] as well as antimony derivatives of carboxylic and phenolic ligands have also been used as antiwear agents or multifunctional additive to lubricants [30]. Thermal degradation of such type of complexes yield highly pure binary antimony sulfide (Sb_2S_3) as final degradation product, which is a kind of semiconductor with its interesting high thermoelectric power. It is a layer-structured direct band gap semiconductor with orthorhombic crystal structure [31] and considered a promising material for solar energy owing to its band gap that covers the range of the solar spectrum [32]. It has been extensively investigated for its special applications as a target material for microwave devices [33], television cameras, switching devices [34], rechargeable storage cells [35] and various optoelectronic devices [36].

In view of the wide range of applications and to keep forward the our research on the design, characterization and development of new biologically active agents containing group 15 metals [37–41], we have synthesized new mixed antimony(III) dimethyldithiocarbamato complexes with oxo or thio donor ligands and characterized by a variety of analytical techniques: physicochemical [melting point, molecular weight determination and elemental analysis (C, H, N, S and Sb)], spectral [UV–Visible, FTIR, far IR, NMR (^{1}H and ^{13}C)], thermal (TGA, DTA and ESI-Mass) analysis and powder X-ray diffraction studies. The free ligands and their antimony complexes have also been screened for their bactericidal and fungicidal effects. These exhibit higher bactericidal and fungicidal effect in comparison to free ligands and some standard antibiotics used.

Experimental

Material and methods

The precursors and complexes form are highly moisture sensitive; therefore, all the experimental manipulations have been carried out under moisture free conditions. Antimony(III) chloride (E. Merck) was purified by distillation before use. Sodium dimethyldithiocarbamate (Aldrich) and ligands [sodium benzoate, sodium thioglycolate, phenol, sodium 1-propanethiolate, potassium thioacetate, sodium salicylate, ethane-1,2-dithiol and disodium oxalate (all Aldrich and E. Merck)] were used as received without further purification. Solvent (hexane, dichloromethane, chloroform, acetonitrile, etc.) were purified by standard methods [42]. *Tris*(*N*,*N*-dimethyldithiocarbamato-*S*,*S*′)antimony(III) and chloro*bis*(*N*,*N*-dimethyldithiocarbamato-*S*,*S*′)antimony(III) were prepared by the method reported in the literature [40,43].

Synthesis of new complexes

*Synthesis of compound **1**–**6** in 1:1 M ratios*

Chloro*bis*(*N*,*N*-dimethyldithiocarbamato-*S*,*S*′)antimony(III) (1.9 g; 4.8 mmol) dissolved in hexane (~40 ml) was added to sodium benzoate **1** (0.7 g; 4.8 mmol) drop-wise. The reaction mixture was refluxed for ~5 h. It was then cooled and precipitated sodium salt was filtered off. The filtrate was reduced under vacuum to obtain the product (Scheme 1).

Compounds (**2**–**6**) were also synthesized by adopting the similar procedure.

*Synthesis of compound **7** and **8** in 2:1 M ratios*

The hexane solution (~40 ml) of chloro*bis*(*N*,*N*-dimethyldithiocarbamato-*S*,*S*′)antimony(III) (2.6 g; 6.6 mmol) was added drop-wise to hexane solution of ethane-1,2-dithiol **7** (0.3 g; 3.3 mmol). The reaction mixture was refluxed for ~5 h followed by filtration. The product was obtained by reducing the solvent under vacuum. The compound **8** have also been prepared by similar procedure. All pertinent analytical and physicochemical data have been summarized in Table 1.

Antimicrobial evaluation

Test micro-organism strains

The ligands used and their synthesized complexes were screened *in vitro* for their antimicrobial activities against four human pathogenic bacterial species [*Staphylococcus aureus* (ATCC 9144) (G^{+ve}), *Bacillus subtilis* (ATCC 6051) (G^{+ve}), *Escherichia coli* (ATCC 9637) (G^{-ve}) and *Pseudomonas aeruginosa* (ATCC 25619) (G^{-ve})] and two plant fungal species [*Aspergillus niger* (ATCC 9029) and *Trichoderma ressie* (ATCC 164)] by using the well diffusion method [37,44]. Standard drugs such as chloramphenicol and terbinafine were used as a reference for antibacterial and antifungal screening respectively.

Method

The compound was dissolved in DMF, to get 200 μg mL^{-1} solution. Further progressive double dilutions were performed to obtain the required concentrations of 100 and 50 μg mL^{-1}. A 0.5 mL solution of the each investigated micro-organisms was added to a sterile nutrient agar (for bacteria)/dextrose agar (for fungi) medium just before solidification, then poured onto sterile Petri dishes (9 cm in diameter) and left to solidify. Using sterile cork borer (6 mm in diameter), three holes (wells) were made in each dish and then 0.1 mL of tested compound dissolved in DMF (50, 100 and 200 μg mL^{-1}) was poured into these holes. Finally the dishes were incubated at 37 °C (24 h) for bacteria and at 30 °C (72 h) for fungi, where clear or inhibition zones were detected around each hole (Fig. S1a and b). Inhibitory activities were measured (in mm) as diameter of the inhibition zones.

A quantity of 0.1 ml DMF alone was used as a control under the same conditions for each organism and by subtracting the diameter of inhibition zone resulting with DMF from that obtained in each case, both antibacterial and antifungal activities can be calculated as a mean of three replicates.

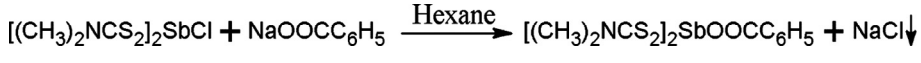

Scheme 1. Synthetic route of compound **1**.

Table 1
Analytical and physicochemical data of *bis*(*N*,*N*-dimethyldithiocarbamato-*S*,*S*′)antimony(III) complexes.

Compound	Yield (%)	Empirical formula M.W. g/mol found (calc.)	M.P. (°C)	Color and state	Elemental analysis (%) found (calc.)				
					C	H	N	S	Sb
1	91	$C_{13}H_{17}N_2O_2S_4Sb$ 481.13 (483.31)	97	Yellow solid	32.22 (32.31)	3.45 (3.55)	5.71 (5.80)	26.35 (26.54)	25.01 (25.19)
2	47	$C_8H_{15}N_2O_2S_5Sb$ 448.51 (453.30)	120[a]	Whitish solid	21.08 (21.20)	3.25 (3.34)	6.11 (6.18)	35.28 (35.37)	26.59 (26.86)
3	45	$C_{12}H_{17}N_2OS_4Sb$ 449.95 (455.30)	–	Yellow semi-solid	31.48 (31.66)	3.56 (3.76)	6.08 (6.15)	28.01 (28.17)	26.61 (26.74)
4	68	$C_9H_{19}N_2S_5Sb$ 434.49 (437.35)	205[a]	Light yellow solid	24.58 (24.72)	4.29 (4.38)	6.38 (6.41)	36.48 (36.66)	27.67 (27.84)
5	86	$C_8H_{15}N_2OS_5Sb$ 433.29 (437.30)	206	Yellow solid	21.81 (21.97)	3.33 (3.46)	6.34 (6.41)	36.36 (36.66)	27.71 (27.84)
6	78	$C_{13}H_{17}N_2O_3S_4Sb$ 495.52 (499.31)	107[a]	Light yellow solid	31.22 (31.27)	3.38 (3.43)	5.49 (5.61)	25.51 (25.69)	24.13 (24.39)
7	82	$C_{14}H_{28}N_4S_{10}Sb_2$ 812.50 (816.57)	137	Yellow solid	20.43 (20.59)	3.41 (3.46)	6.78 (6.86)	39.21 (39.27)	29.65 (29.82)
8	59	$C_{14}H_{24}N_4O_4S_8Sb_2$ 809.22 (812.40)	–	White semi-solid	20.51 (20.70)	2.91 (2.98)	6.81 (6.90)	31.41 (31.58)	29.73 (29.98)

[a] Decomposed.

Analytical methods and physical measurements

Antimony was estimated iodometrically and sulfur was estimated gravimetrically as barium sulfate [45]. Melting points were determined on a B10 Tech India melting point apparatus and are uncorrected. Molecular weights were determined cryoscopically in benzene solution. ^{1}H (at 400 MHz) and ^{13}C (at 100 MHz) NMR spectra were obtained on a Brucker AVANCE-III FT-NMR spectrometer in $CDCl_3$ solution using TMS as an internal standard. Infrared spectra (KBr) were recorded at BX series in the range 4000–400 cm^{-1} and far-IR spectra were recorded as a Nujol mull over CsI disks using a Megna-IR Spectrophotometer-550 instrument in the range 600–50 cm^{-1}. Powder X-ray diffraction studies were performed on diffractometer system XPERT-PRO using Cu Kα radiation at a wavelength of 1.54 Å, ESI-Mass spectra were recorded with a Waters Micromass Q-Tof Micro Mass Spectrometer and thermogravimetric analysis were carried out on Mettler Toledo, model TGA/SDTA 851$_e$.

Results and discussion

Synthesis

Bis(*N*,*N*-dimethyldithiocarbamato-*S*,*S*′)antimony(III) complexes have been synthesized by the replacement reactions of chloro-*bis*(*N*,*N*-dimethyldithiocarbamato-*S*,*S*′)antimony(III) with oxo or thio donor ligands in 1:1 or 2:1 M ratios in refluxing hexane solution for ~5 h (Schemes 1 and 2).

Electronic spectra

The electronic absorption spectral data of these mixed complexes are listed in Table 2 and important characteristic bands were tentatively assigned on the basis of earlier publication [37,39,46]. Three characteristic absorption bands were obtained in the UV spectra. An intense band around 248–261 nm was observed due to the π–π* intramolecular charge transfer transition of the dithiocarbamate group. The NCS group shows π–π* transition as a second band between 300 and 312 nm and third one of low intensity band appeared at 340–360 nm probably due to *n*–π* or charge transfer transition involving the transition of an electron of the lone pair of the sulfur atom to an antibonding π-orbital of dithiocarbamate group. In addition, the electronic spectra of synthesized complexes also show medium to strong intensity absorption bands owing to chromophoric group of the oxo or thio donor ligands. The compound **1**, **2**, **5**, **6** and **8** shows a medium intensity band between 248 and 261 nm due to corresponding carbonyl (C=O) group.

FTIR and far-IR

Three regions in IR spectra of the complexes are of particular importance. The stretching frequency region 1523–1542 cm^{-1} may be assigned to polar CN partial double bond of R_2 NCS_2 [47–49]. Due to asymmetric υ(COO$^-$) and symmetric υ(COO$^-$) group appeared as medium to strong intensity bands at 1714–1719 cm^{-1} and 1251–1262 cm^{-1} respectively, and another band at 1021–1027 cm^{-1} due to υ(C—S) determine the mode of binding of the dithiocarbamate group in the complexes (Table 2). However, the υ(C—S) band in the complexes has been splitted into two signals due to anisobidentate mode of binding [48]. In addition, the bands appearing between 559–568 cm^{-1} and 304–311 cm^{-1} may be assigned to υ(Sb—O) and υ(Sb—S) respectively [37–40,43].

NMR spectral studies

^{1}H NMR

All the spectra of these complexes exhibit the expected pattern without any appreciable shift from the reported data [37–40,43] (Table 3). The CH_3 protons of dimethyldithiocarbamate appeared as a singlet at δ 3.31–3.46. The complex **2** and **6** exhibits a singlet at δ 11.10 and δ 10.93 due to —OH group bearing ligands. In addition, complexes also show expected proton resonance due to corresponding ligand moieties. The ^{1}H NMR spectra of the compounds **1** and **4** are shown in Figs. S2 and S3.

$$2\,[(CH_3)_2NCS_2]_2SbCl + (HSCH_2)_2 \xrightarrow{\text{Hexane}} [(\mu_2\text{-}SCH_2CH_2S)Sb\{S_2CN(CH_3)_2\}_2] + 2\,HCl\uparrow$$

Scheme 2. Synthetic route of compound **7**.

Table 2
UV–Visible (nm) and IR (cm^{-1}) spectral data of *bis*(*N*,*N*-dimethyldithiocarbamato-*S*,*S*′)antimony(III) complexes.

Compound	I Band	II Band	III Band	ν(C—H)	ν(C=O)	ν Asy. (COO^-)	ν(C—N)	ν Sym. (COO^-)	ν(C—S)	ν(Sb—O)	ν(Sb—S)
1	256	310	361	2963	1714	1714	1535	1256	1025	559	308
2	249	304	348	2962	1713	1713	1540	1259	1027	–	306
3	243	309	355	2960	–	–	1530	–	1024	563	311
4	260	312	362	2959	–	–	1542	–	1021	–	308
5	253	300	343	2963	1709	–	1523	1251	1027	–	304
6	261	303	351	2965	1719	1719	1528	1255	1026	561	311
7	255	300	364	2960	–	–	1540	–	1023	–	304
8	248	305	359	2960	1712	–	1535	1262	1024	568	310

Table 3
^1H and ^{13}C NMR spectral data of *bis*(*N*,*N*-dimethyldithiocarbamato-*S*,*S*′)antimony(III) complexes.

Compound	^1H NMR (ppm)	^{13}C NMR (ppm)
1	3.42 (s, 12H—CH_3) 7.38 (t, *J* = 7.2 Hz, 1H, *p*-CH) 7.57 (t, *J* = 7.2 Hz, 1H, *m*-CH) 8.10 (d, *J* = 7.2 Hz, 1H, *o*-CH)	43.7 (—CH_3) 128.4 (Ar C-3,5) 129.9 (Ar C-1) 130.2 (Ar C-2,6) 133.5 (Ar C-4) 170.1 (COO) 200.3 (NCS2)
2	3.41 (s, 12H, —CH_3) 3.69 (s, 2H, —CH_2 acetate) 11.10 (s, 1H, —OH)	24.1 (—SCH_2) 43.9 (—CH_3) 172.4 (—COOH) 200.4 (—NCS_2)
3	3.36 (s, 12H, —CH_3) 7.07 (t, *J* = 7 Hz, 1H, *m*-CH) 7.11 (t, *J* = 7 Hz, 1H, *p*-CH) 7.38 (d, *J* = 7.2 Hz, 1H, *o*-CH)	43.1 (—CH_3) 115.2 (Ar C-2,6) 120.3 (Ar C-4) 129.5 (Ar C-3,5) 156.3 (Ar C-1) 199.5 (—NCS_2)
4	1.02 (t, *J* = 7.4 Hz, 3H, —CH_3 ligand) 1.70 (m, 2H, —CH_2CH_3) 2.65 (t, *J* = 7.2 Hz, 2H, —SCH_2—) 3.40 (s, 12H, —CH_3 of dtc)	12.42 (—CH_3 ligand) 21.15 (—CH_2—) 27.38 (—SCH_2—) 43.83 (—CH_3 of dtc) 200.1 (—NCS_2)
5	2.20 (—CH_3 ligand) 3.31 (—CH_3 of dtc)	32.7 (—CH_3 ligand) 44.1 (–CH_3 of dtc) 196.3 (—CO) 199.8 (—NCS_2)
6	3.40 (s, 12H, —CH_3) 6.85 (t, *J* = 7.4 Hz, 1H, Ar C-3) 6.93 (t, *J* = 8.4 Hz, 1H, Ar C-5) 7.39 (d, *J* = 7 Hz, 1H, Ar C-2) 7.88 (t, *J* = 8 Hz, 1H, Ar C-4) 10.93 (s, 1H, —OH)	43.8 (—CH_3) 114.1 (Ar C-1) 117.3 (Ar C-5) 119.0 (Ar C-3) 131.0 (Ar C-2) 161.6 (Ar C-4) 174.9 (Ar C-6) 199.1 (—NCS_2)
7	3.38 (s, 4H, —SCH_2) 3.62 (s, 12H,—CH_3)	40.8 (—SCH_2) 44.1 (—CH_3) 198.2 (—NCS_2)
8	3.46 (s, 12H, —CH_3)	43.2 (—CH_3) 160.4 (—CO) 198.7 (NCS_2)

dtc: Dimethyldithiocarbamate; Ar: aromatic.

^{13}C NMR

The ^{13}C NMR spectra of dimethyldithiocarbamate moieties show signals at δ 43.1–44.1 due to CH_3 carbon. All these complexes also exhibit a weak signal at δ 198.2–200.4 due to NCS_2 carbon resonance as well as compound **1**, **2**, **4**, **5** and **8** exhibits an expected weak signal between δ 169.83–172.60 due to COO carbon resonance (Table 3).

Powder X-ray diffraction studies

Powder X-ray diffraction pattern for compound **1**, **2** and **4** have been obtained are shown in Figs. 1, S4 and S5 and results summarized in Table 4, S1 and S2. The complexes have been identified as a monoclinic crystal lattice with unit cell volume $V = 400.06 \times 10^{-8}\,cm^{-3}$ (**1**), $V = 1028.02 \times 10^{-8}\,cm^{-3}$ (**2**) and $V = 833.70 \times 10^{-8}\,cm^{-3}$ (**4**). The mean crystallite size can be determined from the full width at half-maximum (FWHM) of the diffraction peaks using Debye–Scherrer formula [50,51]:

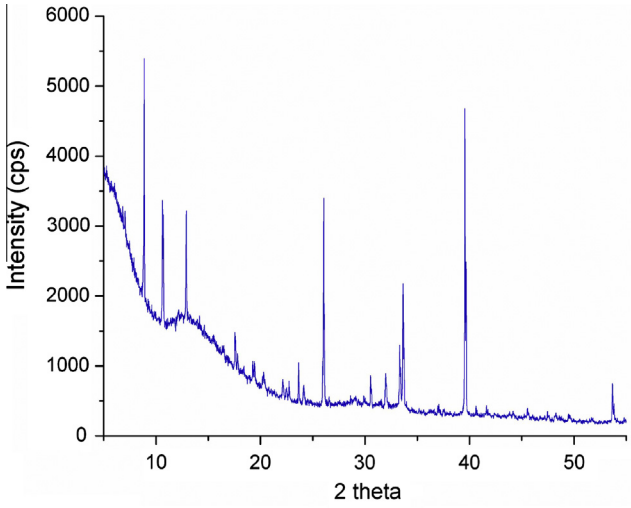

Fig. 1. Powder X-ray diffraction pattern of compound **1**.

$$D = \frac{K\lambda}{B\cos\theta}$$

where D is the particle size, K is a constant whose value is approximately 0.9, λ the wavelength of the X-ray, B the full width at half-maximum and θ is the Bragg angle. The particle size of the complexes found between the range of 11.51–20.82 nm characteristic of nanoparticles. We have synthesizes mixed ligand complexes with characteristic of both type of ligands; therefore, some deviation between the distances (d) may exceed up to 1.08 as observed in Table 4, which shows that synthesized complexes are in multiphase. Interplanar d spacing and unit cell volume of the synthesized complexes were calculated by the formulae [52]:

$$\frac{1}{d^2} = \frac{1}{\sin^2\beta}\left(\frac{h^2}{a^2} + \frac{k^2\sin\beta}{b^2} + \frac{l^2}{c^2} - \frac{2hl\cos\beta}{ac}\right)$$

$$V = abc\sin\beta$$

We have obtained interplaner distances matched with complexes, which are equal and in some cases nearly matches with standard diffraction card JCPDS 72-0022, 43-1978, 01-0303, 36-2000 and 04-0118. Complexes lies under lower symmetry (monoclinic), which is probably due to the complex nature and lone pair of electron present on the metal center, which does not take part in bonding and results in distorted geometry of complexes.

Table 4
The experimental data and the calculated results for powder X-ray diffraction pattern of compound **1**.

S. no.	2 Theta	*d* Spacing (observed)	*d* Spacing (calculated)	Relative intensity (I/I_0)	*h*	*k*	*l*
1	12.89	6.86	5.77	68.81	0	0	1
2	13.09	6.76	5.69	37.99	1	0	0
3	15.51	5.71	4.89	30.85	0	1	1
4	16.49	5.37	4.84	27.66	−1	1	0
5	19.28	4.60	4.60	22.83	0	2	0
6	21.03	4.22	3.60	14.39	0	2	1
7	22.15	4.01	3.58	17.29	1	2	0
8	23.64	3.76	3.38	22.36	−1	2	1
9	24.17	3.68	3.27	15.52	1	1	1
10	26.11	3.41	2.85	72.66	2	0	0
11	27.59	3.23	2.79	10.92	1	2	1
12	28.68	3.11	2.72	12.33	2	1	0
13	29.96	2.98	2.70	12.27	1	3	0
14	30.59	2.92	2.51	18.45	−2	2	1
15	32.05	2.79	2.61	16.99	−1	3	1
16	33.67	2.66	2.19	46.54	−2	2	2
17	34.06	2.63	2.31	9.04	1	3	1
18	35.16	2.55	2.21	8.42	1	1	2
19	37.12	2.42	2.15	9.71	−1	3	2
20	38.27	2.35	2.14	7.46	0	4	1
21	39.67	2.27	2.03	100.00	2	2	1
22	40.61	2.22	1.90	9.15	3	0	0
23	41.79	2.16	1.85	9.30	−3	2	1
24	43.92	2.06	1.82	7.44	2	3	1
25	44.37	2.04	1.83	7.59	1	3	2
26	45.55	1.99	1.83	8.47	−1	4	2
27	46.04	1.97	1.82	6.48	−2	4	1
28	47.57	1.91	1.73	7.48	−1	5	1
29	48.38	1.88	1.62	7.08	1	4	2
30	49.50	1.84	1.64	6.65	2	2	2
31	50.67	1.80	1.75	5.07	0	5	1
32	51.91	1.76	1.46	5.54	−3	3	3

Lattice parameter calculated $a = 6.76$ Å, $b = 9.21$ Å and $c = 6.86$ Å; angle $\beta = 122.73°$. Unit cell volume $V = 400.07 \times 10^{-8}$ cm^{-3}; particle size = 20.82 nm.

ESI-Mass spectral studies

ESI-Mass spectra of three of the complexes, **1**, **2** and **4** have been recorded. ESI-Mass spectrometry is one of the most important tools to determine molecular weight of the complexes [53–55] and to identify the fragments formed during electrospray ionization, which reveal composition and properties of the particular moiety of the complexes. Two important peaks observed in the ESI-Mass spectrum are the base peak and the molecular ion peak (indicating the molecular mass of the complex). In the case of these complexes the molecular ion peak does not appear, which may be due to the pyrolytic decomposition at the relatively high temperature, or due to the fragmentation of molecular ion in the ionization chamber [56]. However, all of the three compounds show the base peak at *m*/*z* 360.7 indicating the fragmentation of metal–ligand bond as well as strong chelating property of the dithiocarbamate than other ligands used. The possible formulae of the fragments and their *m*/*z* ratios are as follows:

Positive-ion ESI-Mass spectra of $[(CH_3)_2NCS_2]_2SbOOCC_6H_5$ (M)

m/*z* (%)[Possible formula of the fragments]: 530.4 (5) $[M+C_3H_9]^+$, 498.4 (4) $[M + CH_3]^+$, 454.3 (5) $[M—C_2H_5]^+$, 417.0 (11) $[M—H_2S_2]^+$, 364.9 (13) $[M—C_6HCOO]^+$, 362.8 (64) $[M—C_6H_3COO]^+$, 360.8 (100) $[M—C_6H_5COO]^+$, 347.1 (23) $[M—C_7H_8COO]^+$, 303.1 (10) $[M—C_{10}H_{17}COO]^+$, 371.0 (26) $[M—C_{10}H_{18}CO_2S]^+$, 257.1 (45) $[M—C_{10}H_{18}CNO_2S]^+$, 239.0 (10) $[M—C_{10}H_{22}CN_2O_2S]^+$, 225.0 (14) $[M—C_{11}H_{24}CN_2O_2S]^+$, 207.0 (6) $[M—C_{10}H_{17}N_2S_3]^+$, 193.0 (8) $[M—C_{11}H_{18}N_2S_3]^+$, 181.0 (6) $[M—C_{10}H_{17}N_2S_3]^+$, 153.4 (17) $[M—C_{13}H_{19}N_2OS_3]^+$.

Positive-ion ESI-Mass spectra of $[(CH_3)_2NCS_2]_2SbSCH_2COOH$ (M)

m/*z* (%)[Possible formula of the fragments]: 419.6 (40) $[M—H_3O_2]^+$, 417.0 (10) $[M—H_5O_2]^+$, 412.9 (4) $[M—C_4H_5]^+$, 360.7 (100) $[M—SCH_2COOH]^+$, 338.3 (5) $[M—C_5H_{12}COO]^+$, 320.3 (4) $[M—C_6H_{16}NO_2]^+$, 305.5 (3) $[M—C_6H_{17}N_2O_2]^+$, 285.0 (4) $[M—C_5H_{18}N_2S_2]^+$, 243.2 (2) $[M—C_6H_{19}N_2OS_2]^+$, 212.2 (2) $[M—C_6H_{16}N_2OS_3]^+$, 200.2 (2) $[M—C_7H_{16}N_2OS_3]^+$, 186.1 (2) $[M—C_8H_{17}N_2O_2S_3]^+$.

Positive-ion ESI-Mass spectra of $[(CH_3)_2NCS_2]_2SbSCH_2CH_2CH_3$ (M)

m/*z* (%) [Possible formula of the fragments]: 421.0 (2) $[M—CH_3]^+$, 417.0 (9) $[M—CH_7]^+$, 393.2 (2) $[M—C_3H_7]^+$, 364.9 (19) $[M—C_5H_{13}]^+$, 360.7 (100) $[M—SCH_2CH_2CH_3]^+$, 332.4 (8) $[M—SC_5H_{13}]^+$, 303.8 (2) $[M—SC_7H_{19}]^+$, 199.5 (3) $[M—C_8H_{17}N_2S_3]^+$, 186.2 (2) $[M—C_9H_{19}N_2S_3]^+$.

Thermogravimetric analysis (TG & DTA)

Thermal behavior of three of the synthesized complexes (**1**, **2** and **4**) has been analyzed in inert atmosphere in a range of 25–600 °C as shown in Table 5. Thermal degradation of the complexes by which we analyze a change in the weight of the substance as a function of temperature or time indicates the formation of antimony sulfide as a final decomposition product [57,58]. It supports to the facts that the synthesized complexes may be used as a single source precursor to obtaining such type of materials having lots of commercial applications.

The TG and DTA curves in Figs. S6, 2 and 3 show two, four and five steps weight losses corresponded to the compounds **1**, **2** and **4**, respectively. Fig. S6 exhibits two steps weight losses. The curve indicates that, the decomposition starts at 70 °C and continues to decompose till 295 °C. This step corresponds to the loss of C_6H_5-COO group and some other organic part of the compound. The expected and observed mass losses are 54.01% and 55.24%, respectively. The final step corresponding to the decomposition of NC part of the dithiocarbamate and subsequent formation of ½ Sb_2S_3, lies in the temperature range 295–400 °C. The total expected and observed mass losses, after complete formation of ½ Sb_2S_3 are 64.77% and 65.17%, respectively. The DTA profile of steps I and II are shown as endothermic peak at 250 and 313 °C.

First step (70–195 °C) of compound **2** (Fig. 2) related to the removal of absorbed water molecule and in second step (195–310 °C) the CH_2COOH and 4 CH_3 groups have been removed with expected (26.27%) and observed (25.68%) mass losses. The third step (310–430 °C) corresponded to the degradation of sulfur atoms. The final step (430–580 °C) indicates the degradation 2 NC groups followed by the formation of ½ Sb_2S_3. The total expected and observed mass losses, after the complete formation of ½ Sb_2S_3 are 66.50% and 67.29%, respectively. The DTA profile of steps I, II, III and IV are shown as endothermic peaks at 176, 275, 333 and 550 °C, respectively.

In the case of complex **4**, we observed five steps weight losses as shown in Fig. 3. First step of decomposition occurs within a range of 75–180 °C with the removal of trapped water. Second step (180–260 °C) deals with the removal of C_3H_7 fragment of thiopropanoate ligand with expected (9.84%) and observed (10.28%) values of mass losses. Third step (260–325 °C) indicates the elimination of 4 CH_3 and S atoms with expected (24.69%) and observed (25.46%) mass losses. The forth step (325–405 °C) corresponded to the removal of 2 S atoms from the 2 NCS residues of third step. The expected and calculated values of mass losses are 14.64 and 14.63%, respectively. Final step, which corresponded to the removal of 2 NC residues of the dithiocarbamate and subsequent conversion of Sb(III) to ½ Sb_2S_3 lies in the temperature range (405–562 °C). The total observed mass loss after the completion of this step was 66.72%, while the expected mass loss was 65.19%. In the DTA curves the decomposition of the ligands represented by the endothermic

Table 5
Thermogravimetric (TG & DTA) data of compounds **1**, **2** and **4**.

Compound	Steps	Decomposition temp. range (°C)	Mass losses (%) found (calc.)	Remaining fragments	DTA_{max} (°C)
1	I	70–295	55.24 (54.01)	2NC + ½ Sb_2S_3	250[d]
	II	295–400	9.93 (10.76)	½ Sb_2S_3[a]	313[d]
2	I	70–195	4.14 (3.98)	–	150[d]
	II	195–310	25.68 (26.27)	2NCS + ½S_3 + ½ Sb_2S_3	275[d]
	III	310–430	25.29 (24.71)	2NC + ½ Sb_2S_3	333[d]
	IV	430–580	12.18 (11.47)	½ Sb_2S_3[b]	550[d]
4	I	75–180	3.69 (4.12)	–	110[d]
	II	180–260	10.28 (9.84)	$C_6H_{12}N_2S_5Sb$	218[d]
	III	260–325	25.46 (24.69)	2NCS + ½ Sb_2S_3	280[d]
	IV	325–405	14.64 (14.53)	2NC + ½ Sb_2S_3	334[d]
	V	405–562	12.65 (11.89)	½ Sb_2S_3[c]	517[d]

[a] Remaining material, found (calc.) = 34.83 (35.14).
[b] Remaining material, found (calc.) = 36.84 (37.46).
[c] Remaining material, found (calc.) = 36.97 (38.87).
[d] Endothermic reaction.

peaks at 228, 280, 334 and 517 °C corresponded to the second, third, fourth and fifth step, respectively.

In vitro antimicrobial studies

To evaluate the antimicrobial activities of free ligands and their antimony(III) complexes [38], these have been screened *in vitro* against four human pathogenic bacterial species [*S. aureus* (ATCC 9144) (G^+), *B. subtilis* (ATCC 6051) (G^+), *E. coli* (ATCC 9637) (G^-) and *P. aeruginosa* (ATCC 25619) (G^-)] (Figs. S7 and S8) and two plant fungal species [*A. niger* (ATCC 9029) and *T. ressie* (ATCC 164)] (Fig. S9) at three different concentrations (50, 100 and 200 μg mL^{-1}).

Chloramphenicol and terbinafine have been used as standard drugs and their activities have been compared with the activities of free ligands and their antimony(III) complexes. A considerable impact of the central metal atom of the complexes has been found against the tested bacterial (Table S3) and fungal species (Table S4).

The results obtained by disc diffusion method indicate that, the synthesized metal complexes have enhanced activities compared to the free ligands, which supports that, the coordination of ligands to the metal center increases the biochemical activities. A comparison has been made between the antimicrobial activities of the free ligands and their metal complexes with chloramphenicol (standard antibacterial drug) and terbinafine (standard antifungal drug) are as follows:

(i) The results showed that, the metal complexes exhibiting higher antibacterial and antifungal activities than the free ligands. It is noticeable here that, Gram-negative bacteria *E. coli* shows resistance to free ligands (**1**–**4** and **6**) and *P. aeruginosa* and *S. aureus* to ligand **1** and **6**.
(ii) It has also been observed that, the free ligands and antimony(III) complexes inhibit the growth of bacteria to a greater extent as the concentration is increased.
(iii) All the complexes showed greater or equal activities against bacterial and fungal species than the standard drugs, chloramphenicol and terbinafine.

Structure elucidation

On the basis of strong intensity bands in the range of 1021–1027 cm^{-1} due to υ(C—S) indicating anisobidentate behavior of

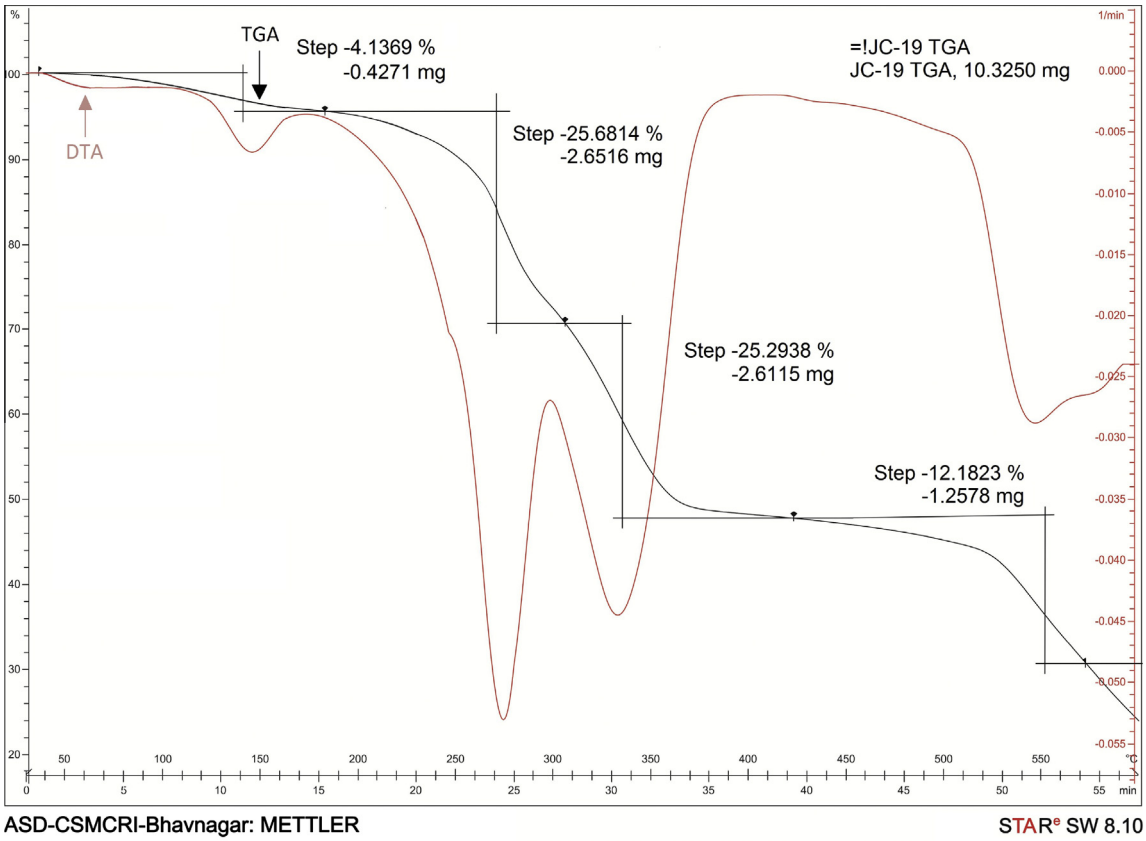

Fig. 2. TG and DTA curves of compound **2**.

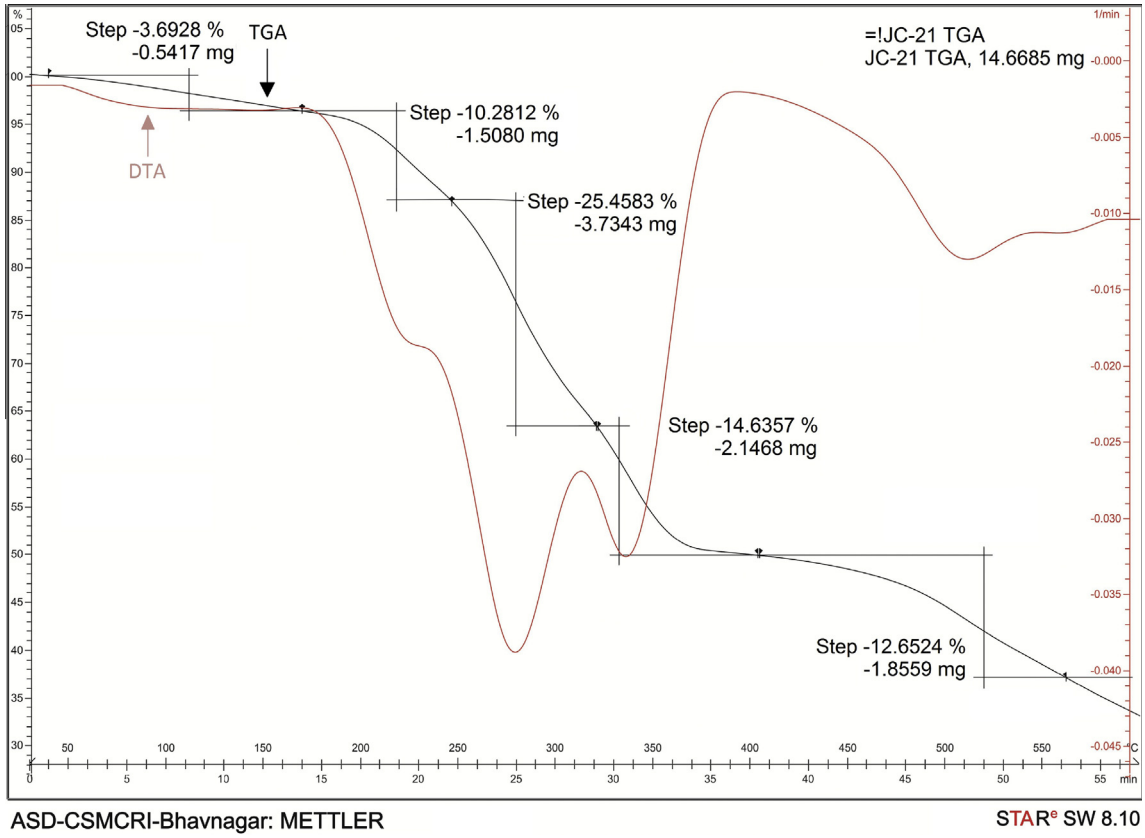

Fig. 3. TG and DTA curves of compound **4**.

dithiocarbamate group and the NMR spectra explaining the structural framework, it may be tentatively concluded that, the complexes adopted distorted octahedral geometry with stereochemically active lone pair of electrons occupying one of the triangular face of octahedra (Fig. 4). In addition, powder X-ray diffraction studies show that, the complexes are crystalline in nature, nano-ranged particle size (11.51–20.82 nm) and having monoclinic crystal system, which supports to distorted octahedral geometry and indicate the lower symmetry of the complexes.

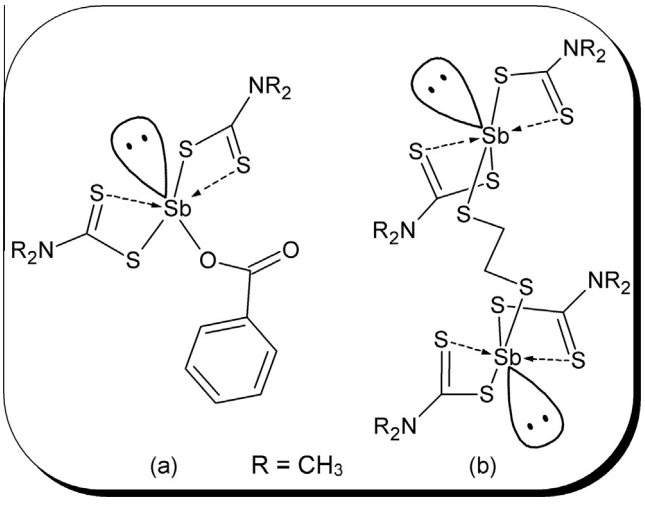

Fig. 4. Proposed structure for (a) *bis*(*N*,*N*-dimethyldithiocarbamato-*S*,*S*′)antimony(III) benzoate **1** and (b) di-μ-ethane-1,2-dithiolato*bis*(*N*,*N*-dimethyldithiocarbamato-*S*,*S*′)antimony(III) **7**.

Conclusion

The mixed *bis*(*N*,*N*-dimethyldithiocarbamato-*S*,*S*′)antimony(III) complexes with oxo or thio ligands have been synthesized and characterized by a number of physicochemical, spectral techniques and thermal analysis as well as the biochemical activity screening test performed against some bacterial and fungal species. It is concluded on the basis of above studies that the complexes adopted distorted octahedral geometry in which the lone pair of electrons occupying one of the triangular face of octahedral, crystalline in nature, nano-ranged particle size with monoclinic crystal system. The ESI-Mass and thermal studies provided fragmentation patterns and final degradation product as highly pure antimony sulfide.

The biochemical screening activity test results that, the complexes are exhibiting higher antibacterial and antifungal activities than the free ligands as well as these showed greater or equal activities than the standard drugs (S.D.) chloramphenicol and terbinafine.

Acknowledgements

The authors thank to University Grant Commission (UGC), New Delhi for financial support [F.39-801/2010(SR)] for the accomplishment of this work. We are also thankful to CSMCRI, Bhavanagr, Gujarat; Sophisticated Analytical Instrumentation Facility (SAIF), Chandigarh and SAIF, Mumbai for TGA/DTA; ESI-Mass and far IR spectral studies, respectively. IISER, Bhopal and UGC–DAE–CSR, Indore are gratefully acknowledged for NMR (^{1}H and ^{13}C) and Powder XRD studies, respectively.

Appendix A. Supplementary material

Supplementary data associated with this article can be found, in the online version, at http://dx.doi.org/10.1016/j.saa.2014.03.054.

References

[1] K.S. Siddiqi, S.A.A. Nami, L. Chebude, Y. Chebude, J. Braz. Chem. Soc. 17 (2006) 107–112.
[2] R. Say, E. Birlik, Z. Erdemgil, A. Denizli, A. Ersoz, J. Hazard. Mater. 150 (2008) 560–564.
[3] N. Unlu, M. Ersoz, Sep. Purif. Technol. 52 (2007) 461–469.
[4] F. Fu, H. Zeng, Q. Cai, R. Qiu, J. Yu, Y. Xiong, Chemosphere 69 (2007) 1783–1789.
[5] Y. Yoshikawa, Y. Adachi, H. Sukurai, Life Sci. 80 (2007) 759–766.
[6] S. Ozkirimli, T.I. Apak, M. Kiraz, Y. Yegenoglu, Arch. Pharmacal Res. 28 (2005) 1213–1218.
[7] F. Shaheen, A. Badshah, M. Gielen, C. Gieck, M. Jamil, D. de Vos, J. Organomet. Chem. 693 (2008) 1117–1126.
[8] V. Alverdi, L. Giovagnini, C. Marzamo, R. Seraglia, F. Bettio, S. Sitran, R. Graziani, D. Fregona, J. Inorg. Biochem. 98 (2004) 1117–1128.
[9] R. Singh, N.K. Kaushik, Spectrochim. Acta A 71 (2008) 669–675.
[10] G. Faraglia, S. Sitran, D. Montagner, Inorg. Chim. Acta 358 (2005) 971–980.
[11] O. Guzel, A. Salman, Bioorg. Med. Chem. 14 (2006) 7804–7815.
[12] P.J. Heard, Prog. Inorg. Chem. 53 (2005) 1–69.
[13] G.D. Thorn, R. Ludwig, The Dithiocarbamates and Related Compounds, Elsevier, Amsterdam, 1981.
[14] S. Cuzzocrea, P.K. Chatterjee, E. Mazzon, L. Dugo, I. Serraino, D. Britti, G. Mazzullo, A.P. Caputi, C. Thiemermann, Brit. J. Clin. Pharmacol. 135 (2002) 496–510.
[15] P.K. Gessner, T. Gessner, Disulfiram and Its Metabolite, Diethydithiocarbamate: Pharmacology and Status in the Treatment of Alcoholism, HIV Infections, AIDS and Heavy Metal Toxicity, Chapman and Hall, London, 1992.
[16] C.L. Raston, A.H. White, J. Chem. Soc., Dalton Trans. (1975) 791.
[17] G.E. Manoussakis, M.L. Kantouri, R.B. Huff, J. Inorg. Nucl. Chem. 37 (1975) 2330.
[18] G. Hogarth, Prog. Inorg. Chem. 53 (2005) 72.
[19] A.H. Neims, D.S. Coffey, L. Hellerman, J. Biol. Chem. 241 (1966) 5941–5948.
[20] V.N. Elokhina, A.S. Nakhmanovich, A.E. Aleksandrova, B.I. Bishnevskii, I.D. Kalikhman, Pharm. Chem. J. 20 (1986) 629–632.
[21] I. Haiduc, Compr. Coordin. Chem. II 1 (2003) 349–376.
[22] W.W. Kenneth, C.L. Houghton, D.L. Sedlak, Anal. Chem. 70 (1998) 4800–4804.
[23] B. Cvek, V. Melacic, J. Taraba, Q.P. Dou, J. Med. Chem. 51 (2008) 6256–6258.
[24] J. Kateva, S.K. Ivanou, J. Polym. Sci. A 17 (1979) 2707–2718.
[25] V.F. Plyusnin, A.V. Kolomeets, V.P. Grivin, S.V. Larinov, H. Lemmetyinen, J. Phys. Chem. A 115 (2011). 1763–1763.
[26] M.D. Regulacio, N. Tomson, S.L. Stoll, Chem. Mater. 17 (2005) 3114–3121.
[27] G. Cantos, C.L. Barbieri, M. Lacomini, P.A. Gorin, L.R. Travassos, Toxicology 180 (2002) 249–256.
[28] M.I. Khan, S. Gul, I. Hussain, M.A. Khan, M. Ashfaq, I.U. Rahma, F. Ullah, G.F. Durrani, I.B. Baloch, R. Naz, Org. Med. Chem. Lett. 1 (2011) 1–7.
[29] G.L. Willingham, Use of Antimony Salt Stabilizers for 3-Isothiazolones. US Patent 5,145,981, 1992 (September 8).
[30] D.J. Phillips, F.L. Oscar, Additions for Lubricants: Mobil Oil. W01995/0199441, 1995 (July 20).
[31] I.H. Kim, Mater. Lett. 43 (2000) 221–224.
[32] L. Chen, W. Zhu, Q. Han, X. Yang, L. Lu, X. Wang, Mater. Lett. 63 (2009) 1258–1261.
[33] J. Grigas, J. Meshkauskas, A. Orliukas, Phys. Status Solidi A 37 (1976) 39–41.
[34] K.Y. Rajpure, C.H. Bhosale, Mater. Chem. Phys. 64 (2000) 70–74.
[35] M.J. Chockaligam, K. Nagaraja, N. Rangarajan, J. Phys. D 3 (1970) 1641–1645.
[36] L.M. Sander, Nature 322 (1986) 789–793.
[37] H.P.S. Chauhan, A. Bakshi, S. Bhatiya, Appl. Organomet. Chem. 24 (2010) 317–325.
[38] H.P.S. Chauhan, S. Bhatiya, A. Bakshi, Spectrochim. Acta A 74 (2009) 67–73.
[39] H.P.S. Chauhan, A. Bakshi, S. Bhatiya, Phosphorus, Sulfur Silicon Relat. Elem. 186 (2011) 345–353.
[40] H.P.S. Chauhan, S. Bhatiya, A. Bakshi, Phosphorus, Sulfur Silicon Relat. Elem. 186 (2011) 511–519.
[41] H.P.S. Chauhan, S. Chourasia, Indian J. Chem. A 34 (1995) 664–665.
[42] J.A. Riddick, W.B. Bunger, Techniques of Chemistry (Organic Solvents), third ed., Wiley InterScience, New York, 1970.
[43] H.P.S. Chauhan, J. Carpenter, S. Bhatiya, A. Bakshi, Phosphorus, Sulfur Silicon Relat. Elem. 188 (2013) 1713–1722.
[44] L. Boyanova, G. Gergova, R. Nikolov, S. Derejian, E. Lazarova, N. Katsarov, I. Mitov, Z. Krastev, J. Med. Microbiol. 54 (2005) 481–483.
[45] A.I. Vogel, A Textbook of Quantitative Chemical Analysis, sixth ed., Saurabh Printers, India, 2008.
[46] H.P.S. Chauhan, S. Bhatiya, Spectrochim. Acta A 97 (2012) 1133–1139.
[47] J. Chatt, L.A. Duncanson, L.M. Venazi, Suom. Kemistil. 29 (1956) 75.
[48] F. Bonati, R. Ugo, J. Org. Met. Chem. 10 (1967) 257–268.
[49] B.F.G. Johnson, K.H. Al-Obalidi, J.A. Mecleverty, J. Am. Chem. Soc. 19 (1969) 1668–1670.
[50] H.P. Klug, L.E. Alexander, X-ray Diffraction Procedures for Polycrystalline and Amorphous Materials, second ed., John Wiley & Sons, New York, 1974.
[51] E. Vallat-Sauvain, U. Kroll, J. Meier, A. Shah, J. Pohl, J. Appl. Phys. 87 (2000) 3137–3142.
[52] B.D. Cullity, Elements of X-ray Diffraction, Addison-Wesley Publishing Company, USA, 1958.
[53] T.S.B. Baul, K.S. Singh, M. Holcápek, R. Jirásko, E. Rivarola, A. Linden, J. Organomet. Chem. 690 (2005) 4232–4242.
[54] L. Machucá, L. Dostál, R. Jambor, K. Handlíř, R. Jirásko, A. Růžička, I. Císařová, J. Holeček, J. Organomet. Chem. 692 (2007) 3969–3975.
[55] D.F. Schoener, M.A. Olsen, P.G. Cummings, C. Basic, J. Mass Spectrom. 34 (1999) 1069–1078.
[56] R.K. Gupta, A.K. Rai, R.C. Mehrotra, V.K. Jain, Polyhedron 3 (1984) 721–728.
[57] H.P.S. Chauhan, A. Bakshi, J. Therm. Anal. Calorim. 105 (2011) 937–946.
[58] V.P. Singh, A. Katiyar, S. Singh, Biometals 21 (2008) 491–501.